

Two-Propagation-Modes and Dual-Band Antenna for Circular Polarized TX/RX Systems at C-Band

Ivan HERRERO-SEBASTIAN, Cesar BENAVENTE-PECES

Dept. of Radio Engineering, Universidad Politecnica de Madrid, Nikola Tesla Street, 28031 Madrid, Spain

i.herrerros@alumnos.upm.es, cesar.benavente@upm.es

Submitted June 30, 2021 / Accepted November 30, 2021

Abstract. *This paper presents a novel slotted array for dual-band and circular-polarized applications. Two different propagation modes within a Substrate Integrated Waveguide (SIW), TE_{10} and TE_{20} , feed at the same time two pairs of slots, aimed at different frequency bands. The pairs are properly placed to be illuminated by an only propagation mode, whereas the magnetic field of the other propagation mode presents a null. Unlike many dual-band slot arrays, this novel antenna holds the same beam tilt for both frequency bands by a new method, which is only feasible through the use of two propagation modes. A dual-mode transition, based on a double microstrip input, allows to excite both propagation modes within the SIW, and it can be fed by a novel single layer dual-band phase shifter with a different shift at each frequency. A square patch is placed over each pair of slots to increase the coupled energy per element, resulting in a low polarization loss and high performance compact antenna at 3.5 GHz and 6 GHz for dual-band TX/RX systems at C-Band.*

Keywords

SIW, phase-shifter, dual-band, circular-polarization, array, slot, C-band, 5G

1. Introduction

In recent years, C-band is being widely used since radio broadcast at this frequency is advantageous for rural and maritime zones, and provides low sensibility to rain. Fixed Satellite Services are placed at this band, 3.4–4.2 GHz for downlink and 5.8–6.4 GHz for uplink, as well as 5G services, where the sub-6 GHz band is being deployed currently at the same operative frequencies. Furthermore, free-licensed services are also located, 3.655–3.695 GHz and 5.15–5.825 GHz.

Moreover, these applications, where a pure linear polarization is hard to keep through the transmission channel, usually use circular polarization. Formerly, satellite services have used circular polarization to avoid polarization shifting through the ionosphere, and the newest fifth generation of mobile communications will move towards the usage of Circular

Polarized (CP) antennas, due to the noticeable enhancement of diversity polarization for multipath channels [1] and being less affected by the user effect [2].

Nowadays, the hardest constraints for novel RF-circuits are the weight and size, since portability is becoming one of the most important features in current communications. Planar microwave circuits and antennas have been used for decades to fulfil these requirements. In the last decade, some of the most important technologies to embed microwave circuits are Gap Waveguides [3] and Substrate Integrated Waveguides (SIW) [4], [5], that allow the implementation of planar waveguides directly on a PCB, easier and less expensive to manufacture than conventional waveguides. In addition, for dual-band and duplex systems, switches are being directly embedded on these transmission lines [6] along with other active elements [7], [8].

One of the most widely used antennas for broadband circular polarized applications are stacked patches [9], [10], usually fed by a strip technology, although patch antennas can be easily implemented in SIW technology too [11], [12]. To set an array, these stand-alone radiators usually require a corporate feeding network, which occupies a non-negligible space and makes the manufacturing more complex and expensive.

Leaky-wave antennas provide a solution to excite several radiators to enhance the antenna gain by using simple serial feeding methods, which take up less space than corporate feeding networks and save complexity. Leaky-wave antennas tend to be linear polarized, however, by modifying the structure of the radiator or the feeding method, circular polarized waves can be also achieved [13], [14].

Rampart lines, where the corners of a transmission line are used as radiating elements, can achieve CP, depending on the shape of the transmission line. This one is usually matched either with a load to perform the travelling wave or by a radiating element [15] to radiate the power left by the line. Likewise, amongst the most used leaky-wave antennas are slotted waveguides or SIW. By etching two orthogonal slots on a SIW, fed by the fundamental mode TE_{10} , the circular polarization can be easily generated [16–20]. More complex forms, such as spiral-shaped slots, can be placed on SIW to achieve a circular polarization too [21].

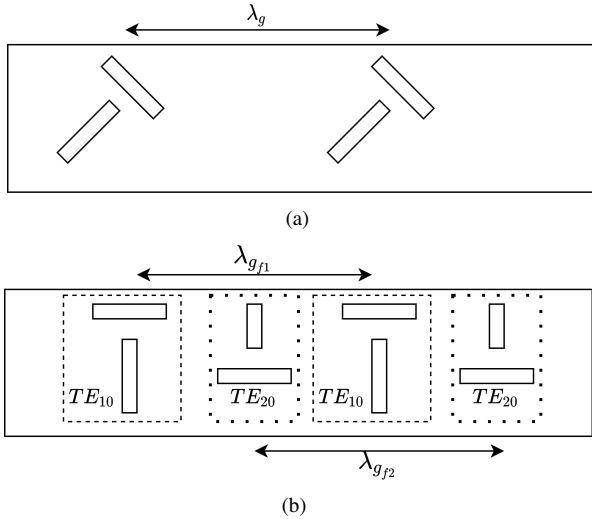


Fig. 1. (a) Conventional CP slotted SIW. (b) Proposed dual-band CP slotted SIW.

In a previous research [22], the authors depicted a novel and very early concept concerning the use of two slot pairs working with two propagation modes. In that research, the proposed slotted SIW array increases the space efficiency with respect to conventional CP-slot arrays. A second pair of slots, working at a different frequency band, is placed in the same SIW. This is achieved by exciting each pair with a different propagation mode, as shown in Fig. 1, through a passive dual-band feeder. In this manner, a magnetic field discrimination on each couple of slots is performed.

That previous development showed some limitations, which are properly solved in the current investigation: a) Each band held a different wavelength, causing overlap or different beam tilts. Now, the wavelengths can be the same by adjusting the SIW width; b) the low mutual interference issue is now properly mathematically described, solved and validated; c) the complexity of constructing a 3-layer board to feed a 2-layer SIW array is avoided by the novel design of a dual-band and dual-phase-shifting single circuit; d) a patch layer is placed over the slots to increase the coupled power per element and achieve compacted arrays; e) several measurements are fulfilled to validate the proposed solution; and f) the results are compared to related CP slotted-works.

By a similar concept of two propagation modes within a SIW, the authors have also demonstrated the design of a dual-linear-polarized cross-shaped-slot array at a single frequency band [23]. However, the current work performs CP at two frequency bands through the usage of two slot pairs, so the design of a novel feeder, as well as a new method to achieve the same beam tilt for each band, must be researched.

The structure of the paper is as follows: Section 2 presents how the surface currents from TE_{10} and TE_{20} work in the slotted SIW to radiate circular polarization, as well as the usage of patches and the method to set the radiator dimensions; Section 3 depicts a novel single layer feeder to excite two propagation modes at two different frequencies within

the SIW; Section 4 presents the manufactured structures and the measurements that validate the presented new concepts; finally, Section 5 sums up the results of the work.

2. Antenna Design

To obtain a 90° phase shift between the longitudinal and transverse magnetic fields, a travelling wave antenna is selected. Aforementioned, when transverse slots are placed on a SIW, fed by the TE_{10} mode, they must be spaced with a distance close to a waveguide wavelength (λ_g) to obtain an almost-broadside radiation pattern, leaving a lot of unused space on the top face and decreasing the area efficiency. However, this novel antenna will place another couple of slots on this unused place, fed by the TE_{20} mode, to radiate at another frequency band and get a dual-band antenna, as depicted by the H-fields in Fig. 2. The resultant radiator occupies the same space as a conventional SIW slot array only based on the propagation of the fundamental mode, and the mutual interference is very low. Tangential surface currents are depicted in Fig. 3, where a low disturbance from the transverse slot, E_i , can be appreciated for TE_{10} .

If the antenna is used on a RX-TX system, the same electrical distance must be used for both slot-pairs to keep the same beam pointing and to avoid slots overlapping. At the central frequency (f_0), for a SIW whose cut-off frequency is f_c , the λ_g for the TE_{n0} mode is given by

$$\lambda_g = \frac{\lambda_{f_0}}{\sqrt{1 - \left(\frac{nf_c}{f_0}\right)^2}}. \quad (1)$$

Hence, both frequency bands, f_1 and f_2 , which are working at different propagation modes, must hold the same wavelength and must satisfy the next equation:

$$\frac{\lambda_{f_1}}{\sqrt{1 - \left(\frac{f_c}{f_1}\right)^2}} = \frac{\lambda_{f_2}}{\sqrt{1 - \left(\frac{2f_c}{f_2}\right)^2}}; f_c = \frac{\sqrt{f_2^2 - f_1^2}}{\sqrt{3}}. \quad (2)$$

For this application, the downlink uses the 3.5 GHz-band fed by the TE_{10} mode, and the uplink, fed by the TE_{20} mode, is set to 6 GHz. If the substrate RO4003C ($\epsilon_r = 3.55$) is selected as the substrate of the SIW, the cut-off frequency which satisfies (2) is set to 2.7 GHz, and both longitudinal via-rows or electric walls must be spaced 28.3mm.

The development of this novel concept, introduced by the authors, is only feasible when two propagation modes exist within the SIW. For example, a research [24] presents a dual-band interleaved slotted SIW antenna only fed by the fundamental propagation mode, but the issue of different beam-tilts at each frequency band is not treated. Axial-Ratio (AR) degradation due to some interference between slot pairs is neither solved.

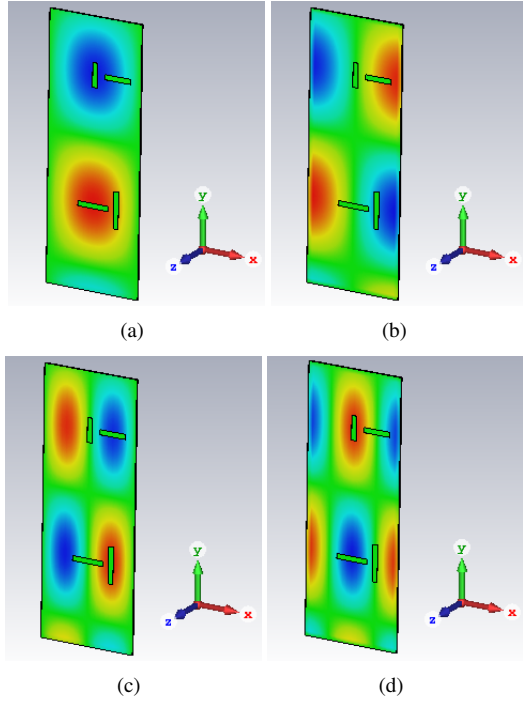


Fig. 2. (a) TE₁₀ H_x, (b) TE₁₀ H_y, (c) TE₂₀ H_x, (d) TE₂₀ H_y.

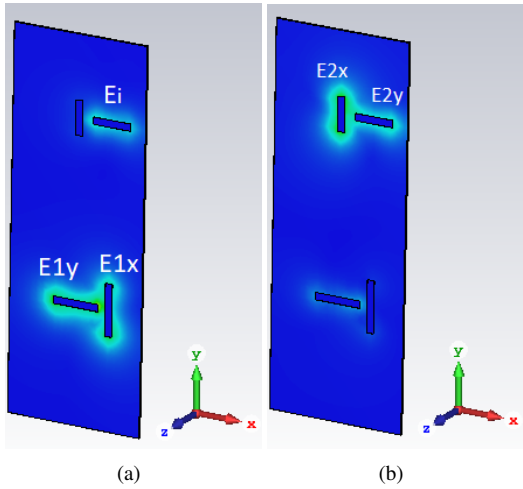


Fig. 3. Max. currents: (a) TE₁₀ J-surface, (b) TE₂₀ J-surface.

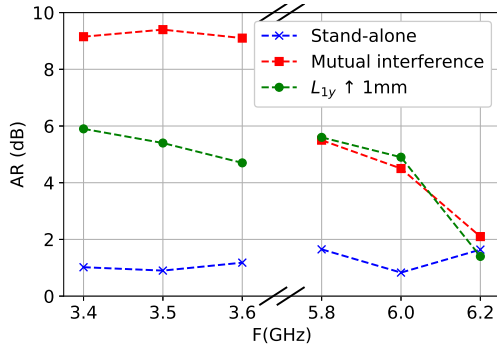


Fig. 4. Axial Ratio: Stand-alone performance (Cross), both pairs on the same SIW (Square) and after correction (Circle).

According to the annotation on Fig. 3, being d is the distance between slot pairs, the radiated field along Z -axis can be expressed as

$$E_{10}(x, y, z) = \hat{x}E_{1x} + \hat{y}(jE_{1y} + E_i e^{j\beta_y d}), \quad z > 0, \quad (3)$$

$$E_{20}(x, y, z) = \hat{x}E_{2x} + \hat{y}jE_{2y}, \quad z > 0. \quad (4)$$

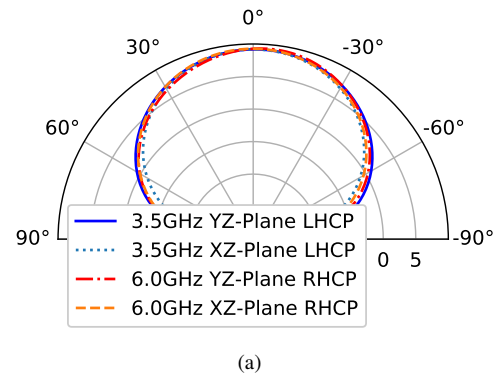
Regarding Fig. 1 and Equation (2), $\lambda_{g_{f_1}}$ and $\lambda_{g_{f_2}}$ are the same, and due to the equal distance between pairs, d is set to $\lambda_g/2$. Hence, Equation (3) can be rewritten as

$$E_{10}(x, y, z) = \hat{x}E_{1x} + \hat{y}j(E_{1y} - E_i), \quad z > 0. \quad (5)$$

E_i purely radiates according to \hat{y} , avoiding the appearance of any non-orthogonal radiation for TE₁₀, but out-of-phase with respect to E_{1y} . To achieve a 0dB-AR, the expected radiation values are $|E_{2y}| = |E_{2x}|$ and $|E_{1x}| = |E_{1y} - E_i|$. When the AR is computed for each stand-alone couple (Figure 4 cross line), two possible values to perform a good Axial-Ratio are set to $L_{1y} = 6.86$ mm and $L_{1x} = 8.2$ mm for TE₁₀ at the lower-band, and $L_{2y} = 7.95$ mm and $L_{2x} = 7.2$ mm for TE₂₀ at the upper-band.

However, when the pairs are placed on the same SIW, the Axial-Ratio at lower-band gets worse due to the influence of E_i . As depicted in (5), L_{1y} must be increased to get back the good AR at lower band. If L_{1y} is increased 1 mm, the Axial-Ratio keeps below 6 dB, as depicted in Fig. 4, and the result validates the concept predicted in (5).

From now on, a layer of resonant patches will be placed 3 mm over each pair to increase the radiated power per slot and obtain a compact wave-travelling antenna. At 6 GHz, a 17.5 mm side-length square patch is selected. Regarding the lower band, the resonant length at 3.5 GHz is 32.5 mm. However, to decrease the interference produced by J_x in the patches, as depicted in (5) for the TE₁₀ mode, the patch width is increased 1.5 mm. Figures 5 and 6 present the performance and stack-up of the proposed dual-band and circular-polarized single-element, respectively. Although 3dB-AR is usually set as reference level, some works present that an AR value between 4~5 dB at some frequencies can also provide average CP performances with a low impact at sub-6 GHz services [25], such as mobile [26] and satellite [27] ones.



(a)

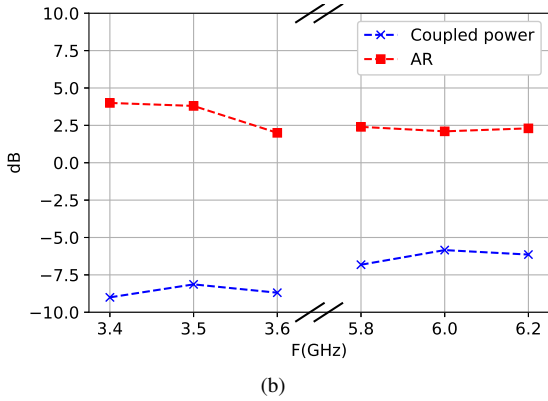


Fig. 5. (a) Single-element with patches: Radiation pattern, (b) AR and efficiency within operative bands.

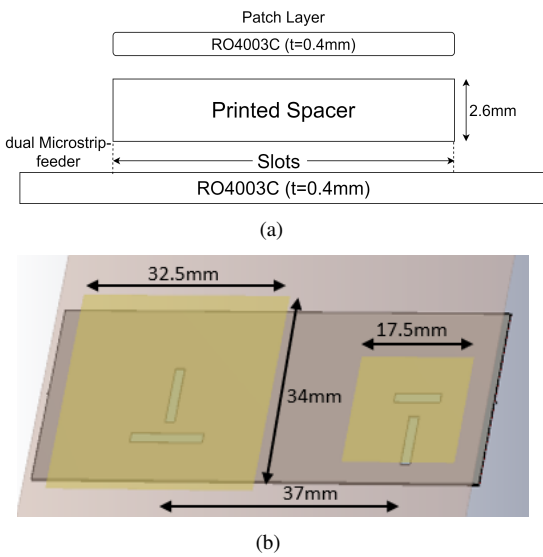


Fig. 6. (a) Antenna Stack-Up, (b) Single element: 3D model.

3. Antenna Feeder Design

Unlike the conventional strip-to-SIW single transitions, which are unable to excite TE₂₀, the proposed feeding method is composed of two microstrip transitions, mirrored from the SIW centre, as presented in Fig. 7. Depending on the phase difference between inputs, TE₁₀ (In-phase signals) or TE₂₀ (Out-of-phase signals) will excite the SIW. Furthermore, CP can be switched between LHCP and RHCP by exciting the SIW from either the upper-side or the lower-side. The Circular Polarization orientation can be also modified by mirroring, from the SIW centre, either the longitudinal slot for TE₁₀ or the transverse one for TE₂₀.

This kind of feeding method can be seen as a Doherty structure. First, the signal is split to apply a determined phase shifting to each branch before the amplification stage. Later, the signal is combined within the radiating structure when the propagation mode is formed, improving the maximum output power and the linearity of the gain blocks.

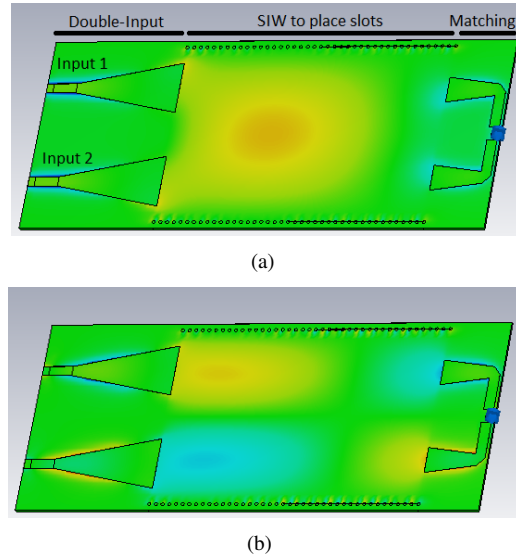


Fig. 7. Dual-band feeding method: (a) TE₂₀, (b) TE₂₀.

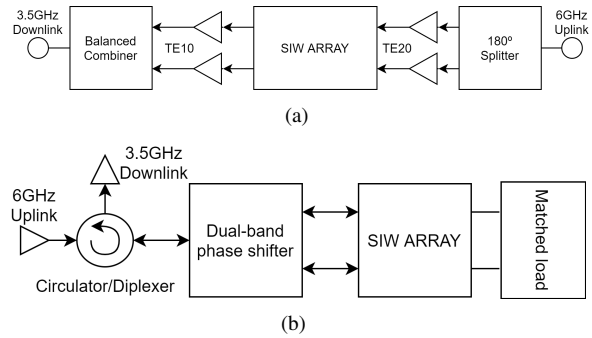


Fig. 8. (a) Double feeding method, (b) Single feeding method.

Two possible methods to feed this transition are feasible and are depicted in Fig. 8. First, Figure 8(a) focuses on a full duplex system, where LHCP is used for RX and RHCP for TX, and each band holds its own feeder. Usually, a Wilkinson-splitter could be used for TE₁₀ and a RatRace splitter can provide a power splitting with 180° phase difference for TE₂₀.

However, unlike the previous method, the novel structure on Fig. 8(b) uses a single feeding circuit to perform a dual-band system. It could also act as a transceiver if a circulator or diplexer is used to split TX and RX frequency bands from the same port. Hence, instead of using a complex multi-layer feeder [22] or interlayer divider and combiner stages, this paper is going to introduce a novel feeding method to design a dual-band phase-shifter to excite two propagation modes at different bands on a single layer circuit.

By using two SIWs of different length and width, the dual-band performance to excite the antenna can be achieved. Let be l_i the length of each SIW, and w_i the correspondent width, the equation system to be solved by a Least-Mean-Square method is defined by (6) and (7).

$$\frac{2\pi}{\lambda_g(w_1, f_1)} l_1 - \frac{2\pi}{\lambda_g(w_2, f_1)} l_2 = 0, \quad (6)$$

$$\frac{2\pi}{\lambda_g(w_1, f_2)} l_1 - \frac{2\pi}{\lambda_g(w_2, f_2)} l_2 = \pi. \quad (7)$$

If some size limitation exists, and any parameter has to be fixed or bounded, Figure 9 shows the proposed structure and the maximum dimensions with respect to the ratio between w_1, w_2 and the cut-off width w_c for the lowest operative frequency. For fixed widths $w_1 = 30$ mm and $w_2 = 24$ mm, the resultant lengths are $l_1 = 27.8$ mm and $l_2 = 44.6$ mm. Figure 10 shows the performance of the dual-phase shifter. The theoretical performance, as well as the simulation results, are compared to a simple 180° splitter such as the RatRace circuit, for the upper band. Despite the simplicity and good accommodation of the dual-phase-shifter, a conventional Ratrace can provide higher phase-bandwidth at the upper-band.

4. Experimental Results and Validation

The two novel electromagnetic structures introduced in this work, the antenna and its feeding circuit, have been manufactured, measured, and tested. The CP dual-band single-radiator element with the proposed double-feeding method is presented in Fig. 11, the dual-band phase shifter performance in Fig. 12 and the measured AR and RL in Fig. 13. The dual-phase shifter and slot boards are manufactured separately, then the slots are placed on the bottom layer of the phase-shifter and their double microstrip feeders are connected through a via. Later, a PLA printed spacer is glued to the board and the patch layer is screwed to them.

The dual-band-phase-shifter achieves an out-of-phase shifting for the upper band, to feed TE_{20} mode, from 5.6 to 6.3 GHz with a phase error of $\pm 10^\circ$, as well as from 3.45 to 3.52 GHz at the lower band, where it exhibits a perfect in-phase combination very close to 3.5 GHz. For these frequency bands, when a single antenna (two slot pairs with their corresponding patches) is fed by the novel phase shifter, the polarization losses are kept below 0.5 dB (*AxialRatio* < 6 dB) as presented in Fig. 13.

In addition, a dual-band 3-element array is also manufactured and measured, with the dual-band and dual-phase-shifting circuit as the antenna feeder, to validate the identical wavelength concept expressed in (2). Figure 14 shows the array made by six equidistant patches, three per frequency-band, and Figure 15 the performed AR and gain. The obtained broadside radiation at both central frequencies and the beam-squint along the frequency bands are depicted in Fig. 16. Axial-Ratio and realized gain present a good match between measurement and simulations. According to these values, the presented work is compared to other related CP-slot-Arrays in Tab. 1.

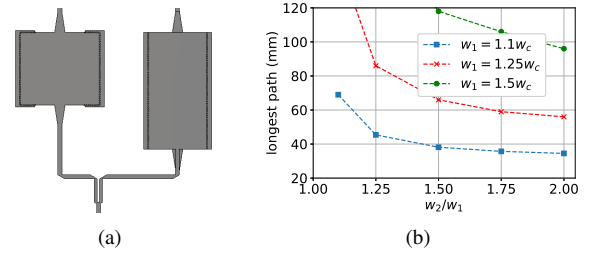


Fig. 9. (a) Dual-Band and dual-phase-shifter structure, (b) Maximum lengths according to SIW widths.

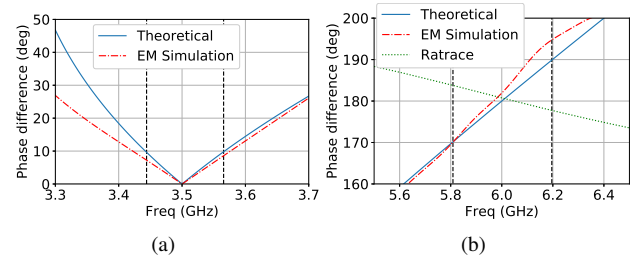


Fig. 10. Phase balance for (a) TE_{10} , (b) TE_{20} .

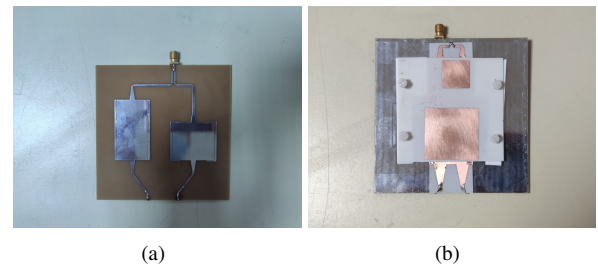


Fig. 11. (a) Top layer: Dual-band and dual-shifting Phase-shifter, (b) Bottom layer: Screwed patch layer over the slots.

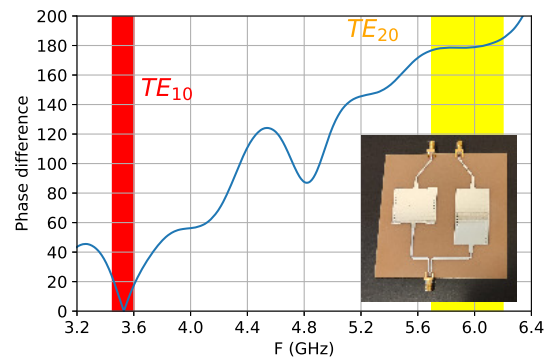


Fig. 12. Dual-band and dual-shifting phase-shifter performance.

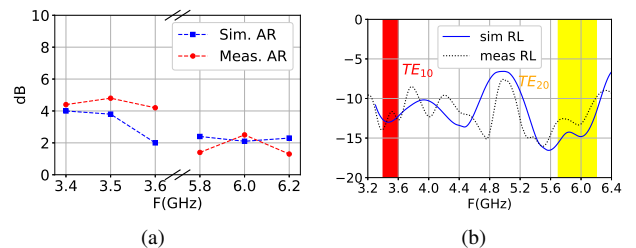


Fig. 13. Dual-band and dual-CP single-element: a) Axial ratio within operative bands, b) Return loss.

Work	Type	f_0 [GHz]	AR - BW [%]	Same beam-tilt	Gain [dBiC]	Size [λ_0 @ upper band]
[28]	Single SIW	3	16	N.A ¹	10 ~ 12	0.8×4.4
[17]	Single SIW and patches	45	11.6	N.A ¹	17.1	4.4×4.4
[16]	Single SIW	12	7.4	N.A ¹	28	35.8×11.6
[21]	double HM-SIW	5.6 9	linear 6.6	No	13.3 14	1.8×8.8
[24]	Single SIW ²	19.2 29.5	11 5.8	No	-	-
[29]	Waveguide with SRR ³	8.5 10	3 linear	Yes	6 ~ 8 7	$0.76 \times 3.3 \times 0.3$
[30]	Single SIW	9.8 14.8	linear 18	No	4 ~ 8 8 ~ 10	1.48×10.85
This	Single SIW and patches	3.5 6	5.7 ⁴ 6.6 ⁴	Yes	5.5 ~ 7.5 5.5 ~ 8.5	0.7×4.5

¹ Not Applicable since works are single-band

² Only simulation

³ SRR: Split Ring Resonator

⁴ Unlike the 3dB-AR level within BW of related works, the presented one shows some frequencies where AR raises up to 4dB. Polarization loss worsens, from 0.1 to 0.2 dB, and XPD from 15 to 13 dB.

Tab. 1. Comparison with related Circularly Polarized LWA slot-Arrays.

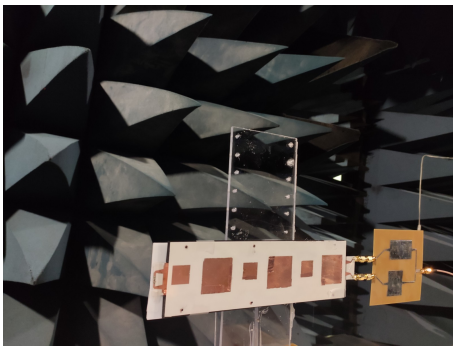


Fig. 14. Manufactured array.

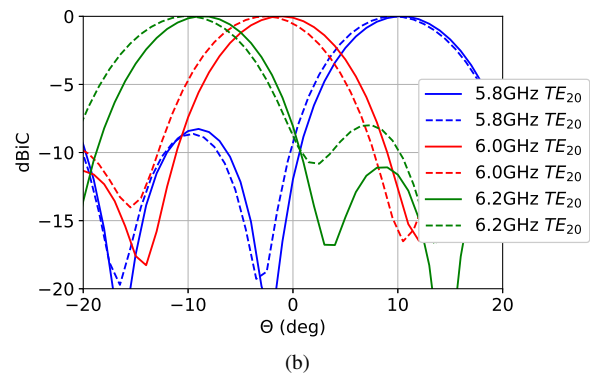
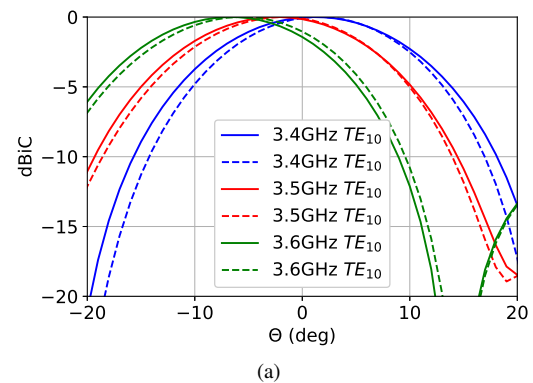


Fig. 16. (a) LHCP radiation pattern at lower band, (b) RHCP radiation pattern at upper band.

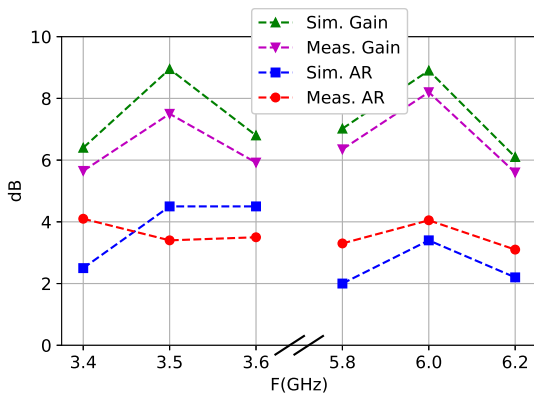


Fig. 15. Axial-Ratio and realized gain within operative bands.

Many dual-band works based on the use of slots can only achieve circular polarization at one only frequency band, and most of dual-band investigations do not solve the issue of different beam-tilts at each frequency band. Even though the proposed work does not provide the widest bandwidth,

it shows the circular polarization performance at both bands, and the beam-tilts can be controlled. Moreover, the proposed antenna also shows a good area efficiency when the resulting gain and size are compared to the related developments.

5. Conclusion

This paper introduces a novel method to develop circular-polarization slot array antennas, which improves the implementation size efficiency over conventional arrays with linear slots. Due to the usage of two propagation modes, magnetic-field diversity can be achieved for two frequency bands in the same Substrate Integrated Waveguide, as well as the same waveguide-wavelength for both bands. Hence, it is worth highlighting the most relevant properties of the resulting antenna: Circular polarization, dual-band, same beam-tilt and independence tuning. In addition, two feeding methods have been presented and analysed. The first one is based on using two splitters, one of them is phase-balanced, and the second one is 180°-shifted, to feed the TE₁₀ and TE₂₀ modes, respectively. Afterwards, a novel dual-band and dual-shift phase-shifter, with different shifting at each frequency and based on the SIW technology, was introduced to make easier the excitation of both modes through a single-layer circuit. The radiator and the dual phase-shifter circuits were manufactured to demonstrate and validate the feasibility of the presented novel concepts, as well as their good Axial Ratio, phase balance, and identical beam pointing at both bands.

References

- [1] MANABE, T., MIURA, Y., IHARA, T. Effects of antenna directivity and polarization on indoor multipath propagation characteristics at 60 GHz. *IEEE Journal on Selected Areas in Communications*, 1996, vol. 14, no. 3, p. 441–448. DOI: 10.1109/49.490229
- [2] SYRYTSIN, I., ZHANG, S., PEDERSEN, G. F., et al. User effects on the circular polarization of 5G mobile terminal antennas. *IEEE Transactions on Antennas and Propagation*, 2018, vol. 66, no. 9, p. 4906–4911. DOI: 10.1109/TAP.2018.2851383
- [3] RAJO IGLESIAS, E., EBRAHIMPOURI, M., QUEVEDO TERUEL, O. Wideband phase shifter in groove gap waveguide technology implemented with glide-symmetric holey EBG. *IEEE Microwave and Wireless Components Letters*, 2018, vol. 28, no. 6, p. 476–478. DOI: 10.1109/LMWC.2018.2832013
- [4] WANG, J., LIU, Y., HOU, Y., et al. Design of gap waveguide PMC packaging for a SIW power combiner. In *IEEE Electrical Design of Advanced Packaging and Systems Symposium (EDAPS)*. Haining (China), 2017, p. 1–3. DOI: 10.1109/EDAPS.2017.8276972
- [5] BARIK, R. K., CHENG, Q. S., PRADHAN, N. C., et al. A compact SIW power divider for dual-band applications. *Radioengineering*, 2020, vol. 29, no. 1, p. 94–100. DOI: 10.13164/re.2020.0094
- [6] TAYEBPOUR, J., AHMADI, B., FALLAHZADEH, M., et al. A waveguide switch based on contactless gap waveguide technology. *IEEE Microwave and Wireless Components Letters*, 2019, vol. 29, no. 12, p. 771–774. DOI: 10.1109/LMWC.2019.2950164
- [7] PECH, P., KIM, P., JEONG, Y. Microwave amplifier with substrate integrated waveguide bandpass filter matching network. *IEEE Microwave and Wireless Components Letters*, 2021, vol. 31, no. 4, p. 401–404. DOI: 10.1109/LMWC.2021.3059859
- [8] DER SPUY, T. V., STANDER, T. An X-band cross-coupled SIW cavity VCO. In *European Microwave Conference (EuMC)*. Utrecht (Netherlands), 2021, p. 100–103. DOI: 10.23919/EuMC48046.2021.9338009
- [9] SU, W., LI, J., LIU, R.-H. A compact double-layer wideband circularly polarized microstrip antenna with parasitic elements. *International Journal of RF and Microwave Computer-Aided Engineering*, 2021, vol. 31, no. 1, p. e22471. DOI: 10.1002/mmce.22471
- [10] ZHU, X. W., GAO, J., CAO, X. Y., et al. A novel low-RCS and wideband circularly polarized patch array based on metasurface. *Radioengineering*, 2019, vol. 28, no. 1, p. 99–107. DOI: 10.13164/re.2019.0099
- [11] HO, A. T., PISTONO, E., CORRAO, N., et al. Circular polarized square slot antenna based on slow-wave substrate integrated waveguide. *IEEE Transactions on Antennas and Propagation*, 2021, vol. 69, no. 3, p. 1273–1282. DOI: 10.1109/TAP.2020.3030933
- [12] CHEN, H., SHAO, Y., ZHANG, Y., et al. A millimeter-wave triple-band SIW antenna with dual-sense circular polarization. *IEEE Transactions on Antennas and Propagation*, 2020, vol. 68, no. 12, p. 8162–8167. DOI: 10.1109/TAP.2020.2996806
- [13] BUI, C. D., NGUYEN TRONG, N., NGUYEN, T. K. A planar dual-band and dual-sense circularly polarized microstrip patch leaky-wave antenna. *IEEE Antennas and Wireless Propagation Letters*, 2020, vol. 19, no. 12, p. 2162–2166. DOI: 10.1109/LAWP.2020.3026067
- [14] AGARWAL, R., YADAVA, R. L., DAS, S. A multi-layered SIW based circularly polarized CRLH leaky wave antenna. *IEEE Transactions on Antennas and Propagation*, 2021, vol. 69, no. 10, p. 6312–6321. DOI: 10.1109/TAP.2021.3082618
- [15] PAN, Y., DONG, Y. Circularly polarised microstrip line leaky-wave antenna terminated with patch. *IET Microwaves, Antennas Propagation*, 2020, vol. 14, no. 12, p. 1331–1336. DOI: 10.1049/iet-map.2020.0330
- [16] KAZEMI, R., YANG, S., SULEIMAN, S. H., et al. Design procedure for compact dual-circularly polarized slotted substrate integrated waveguide antenna arrays. *IEEE Transactions on Antennas and Propagation*, 2019, vol. 67, no. 6, p. 3839–3852. DOI: 10.1109/TAP.2019.2905682
- [17] LI, C., LIU, P., ZHU, X.-W., et al. A SIW-based wideband circularly polarized 4x4 patch array antenna in 45 GHz band. In *12th UK-Europe-China Workshop on Millimeter Waves and Terahertz Technologies (UCMMT)*. London (UK), 2019, p. 1–4. DOI: 10.1109/UCMMT47867.2019.9008312
- [18] MONTISCI, G. Design of circularly polarized waveguide slot linear arrays. *IEEE Transactions on Antennas and Propagation*, 2006, vol. 54, no. 10, p. 3025–3029. DOI: 10.1109/TAP.2006.882201
- [19] CHEN, P., HONG, W., KUAI, Z., et al. A substrate integrated waveguide circular polarized slot radiator and its linear array. *IEEE Antennas and Wireless Propagation Letters*, 2009, vol. 8, p. 120–123. DOI: 10.1109/LAWP.2008.2011062
- [20] PAVONE, S. C., CASALETTI, M., ALBANI, M. Automatic design of a RHCP linear slot array in substrate integrated waveguide. In *12th European Conference on Antennas and Propagation (EuCAP)*. London (UK), 2018, p. 1–3. DOI: 10.1049/cp.2018.1115
- [21] RUDRAMUNI, K., MAJUMDER, B., KANDASAMY, K. Dual-band dual-polarized leaky-wave structure with forward and backward beam scanning for circular polarization-flexible antenna application. *Microwave and Optical Technology Letters*, 2020, vol. 62, no. 5, p. 2075–2084. DOI: 10.1002/mop.32285
- [22] HERRERO-SEBASTIAN, I., BENAVENTE-PECES, C. Dual-band circular polarized slot array antenna in substrate integrated waveguide using two propagation modes for communication satellites transceivers. *Progress In Electromagnetics Research Letters*, 2019, vol. 86, p. 137–143. DOI: 10.2528/PIERL19070104

- [23] HERRERO-SEBASTIAN, I., BENAVENTE-PECES, C. A novel two-propagation-modes dual-polarized slotted-SIW antenna for 5G and sub-6GHz services. *International Journal on Communications Antenna and Propagation (IRECAP)*, 2021, vol. 11, no. 3, p. 147–155. DOI: 10.15866/irecap.v11i3.20810
- [24] KALIALAKIS, C., GEORGIADIS, A. A dual band circularly polarized SIW interleaved antenna array. In *10th European Conference on Antennas and Propagation (EuCAP)*. Davos (Switzerland), 2016, p. 1–4. DOI: 10.1109/EuCAP.2016.7481864
- [25] MADDIO, S. A compact two-level sequentially rotated circularly polarized antenna array for C-band applications. *International Journal of Antennas and Propagation*, 2015, vol. 2015, p. 1–10. DOI: 10.1155/2015/830920
- [26] FARASAT, M., THALAKOTUNA, D. N., HU, Z., et al. A review on 5G sub-6 GHz base station antenna design challenges. *Electronics*, 2021, vol. 10, no. 16, p. 1-20. DOI: 10.3390/electronics10162000
- [27] ARNAUD, E., HUITEMA, L., CHANTALAT, R., et al. Circularly polarized ferrite patch antenna for LEO satellite applications. *International Journal of Microwave and Wireless Technologies*, 2020, vol. 12, no. 4, p. 332–338. DOI: 10.1017/S1759078719001429
- [28] CHEN, S., KARMOKAR, D. K., QIN, P., et al. Polarization-reconfigurable leaky-wave antenna with continuous beam scanning through broadside. *IEEE Transactions on Antennas and Propagation*, 2020, vol. 68, no. 1, p. 121–133. DOI: 10.1109/TAP.2019.2935122
- [29] CHANDRA, A., DAS, S. Polarizer superstrate and SRR-loaded high-gain dual band dual polarized waveguide slot array antenna. *International Journal of RF and Microwave Computer-Aided Engineering*, 2018, vol. 28, no. 4, p. e21225. DOI: 10.1002/mmce.21225
- [30] ZHANG, Q., ZHANG, Q., LIU, H., et al. Dual-band and dual-polarized leaky-wave antenna based on slotted SIW. *IEEE Antennas and Wireless Propagation Letters*, 2019, vol. 18, no. 3, p. 507–511. DOI: 10.1109/LAWP.2019.2895339

About the Authors ...

Ivan HERRERO-SEBASTIAN (corresponding author) was born in Zaragoza, Spain, in 1993. He received his Bachelor's in Telecommunication Engineering from Zaragoza University in 2015, and his M.Sc. in RF and Electronic Systems from Technical University of Madrid in 2016. His research interests include RF circuits, antennas and signal processing. He started the Ph.D. studies in 2017 and has published some papers in international journals about RF design using SIW technology. Besides the Ph.D. studies, he is working with international companies for RF and antenna design in the aero-space field.

Cesar BENAVENTE-PECES was born in Madrid, Spain, in 1967. He received his Ph.D. in Telecommunications Engineering in 1999 from Technical University of Madrid. He is Professor at the same university in the Circuits and Systems Engineering Department, at the Faculty of Telecommunications. He is the author of more than one hundred papers published in relevant international journals, conference proceedings, and book chapters. His research interests are related to digital signal processing in communication systems, software radio systems and MIMO communication systems. Prof. Benavente-Peces has served as Conference Chair for SENSORNETS and PECCS, and Guest Editor. He has led several projects funded by regional, national, and international governments, and contracts with the industry.